J Mater Sci (2014) 49:7418–7424
DOI 10.1007/s10853-014-8442-6

Toward *p*-type conduction in Cs-doped ZnO: an eco-friendly synthesis method

Veena Ragupathi · Srimathi Krishnaswamy · Senthilkumaar Sada · Ganapathi Subramanian Nagarajan · Sudarkodi Raman

Received: 5 May 2014 / Accepted: 2 July 2014 / Published online: 22 July 2014

Abstract An alcohol-free, eco-friendly technique was adapted for the synthesis of undoped ZnO and Cs-(cesium) doped ZnO nanoparticles (NPs). The effect of annealing and dopant concentration on its structural and optical properties was investigated. X-ray diffraction results confirmed the formation of polycrystalline hexagonal wurtzite structure and enhanced crystallinity was observed for 1 mol%: Cs-doped ZnO NPs. Scanning electron microscopy results revealed triangular-shaped NPs and increase in the crystallite size is noticed with increase in dopant concentration. UV–visible results showed shift in the band edge toward higher wave length side with increasing Cs concentration. Reduction in bandgap was observed for Cs-doped ZnO NPs, due to quantum confinement effect. Transmittance value increased to 86 % with the inclusion of Cs in ZnO lattice. Room temperature photoluminescence analysis of Cs-doped ZnO NPs reveals bandedge emission along with 450 nm emission due to Zn vacancy and Zn interstitial defects. Electrical measurements confirmed the realization of *p*-type conductivity in Cs-doped ZnO NPs with a carrier concentration of $1.3 \times 10^{18}/\text{cm}^3$.

V. Ragupathi · S. Krishnaswamy · S. Raman (✉)
Centre for Clean Energy and Nano Convergence (CENCON), Hindustan University, Padur, Kelambakkam, Chennai, India
e-mail: rsudarkodi@hindustanuniv.ac.in

S. Sada
Building No. 8, Marutham Nagar Extension, Vadavalli, Coimbatore, India

G. S. Nagarajan
Quantum Functional Semiconductor Research Centre (QSRC), Nano Information Technology Academy (NITA), Dongguk University, 26 Phildong 3ga, Chunggu, Seoul 100-715, South Korea

Introduction

Short-wavelength optical devices are used in a variety of applications such as optical recording displays, optical storage devices, medical appliances, and measuring instruments [1]. Recently, lot of research has been focused on realization of practical application from cheap and efficient semiconductor based short-wavelength optoelectronic devices [2, 3]. Zinc oxide (ZnO) is a versatile semiconductor material and has attractive properties like nontoxicity, environment-friendly, wide band gap (3.2 eV), and a large exciton binding energy of 60 meV at room temperature [4, 5]. Zinc oxide is of great interest due to its strong UV photo response, established synthesis methods, chemical and thermal stability [6]. To obtain better ZnO-based optoelectronic devices, high quality *n*- and *p*-type ZnO is needed. Generally, ZnO is a native *n*-type semiconductor material and to acquire *p*-type conduction in ZnO is challenging [7]. The difficulty in *p*-type doping in ZnO is mainly due to self-compensation by donor like native defects, low dopant solubility, and less stability [8, 9].

p-type ZnO can be achieved by the substitution of group I element in the Zn site and group V element in oxygen site. Recently, group I elements such as Li, Na, and K have been found to be potential dopants in ZnO [10, 11]. However, when elements of smaller ionic radius like Li were doped with ZnO, a less stable *p*-type semiconductor was formed, because Li behaves like a shallow acceptor/reactive donor [12]. K and Na (bigger cationic radius) ions show stable *p*-type conductivity as they behave like deep acceptors [13]. Similarly cesium possess higher ionic radius (174 pm) when compared to other group I elements, therefore may provide a better *p*-type stability than other group I elements. On the contrary, very few reports on

optical and electrical properties of Cs-doped ZnO NPs have been published so far [14, 15].

Also, a large number of physical and chemical methods are available to synthesize undoped and doped ZnO NPs [16, 17]. Compared with chemical and physical methods, green synthesis methods have received a lot of attention due to low cost, simplicity, versatility, and scalability [18]. "Green synthesis" of nanoparticles (NPs) makes use of environmental friendly, non-toxic, and safe reagents and therefore neither high temperature, pressure nor toxic chemicals are required [19]. Hence, in the present paper, a green approach is adopted for the synthesis of ZnO NPs and its effect on *p*-type conduction in Cs-doped ZnO NPs have been reported for the first time in lieu of our knowledge. In this manuscript effort has been made to demonstrate the structural, optical, and electrical properties of Cs-doped ZnO NPs.

Experimental

Zinc nitrate hexahydrate (98 % Sigma Aldrich) and cesium nitrate (99.99 %, Alfa Aesar) were used as the precursors for synthesis of ZnO NPs. Green-solvent was extracted from *citrus* × *sinensis* peel. The brief synthesis of bio-extract was mentioned in the previous work [20]. For the synthesis of undoped ZnO and Cs-doped ZnO (1 and 3 mol%) NPs, appropriate amounts of precursors were dissolved in double distilled water. The bio-extract was added to the precursor solution drop by drop over a period of 6 h with constant stirring. The precursor solution was stirred overnight at constant speed, and then the solution was heated to 60 °C for 2 h to get a homogeneous and transparent sol. The transparent gel was dried at 150 °C for 12 h. The dried white precipitate was calcined at 500 °C for 2 h to obtain ZnO and Cs-doped ZnO NPs. As grown Cs:ZnO NPs results were reported earlier [21]. In the present study in order to enhance crystallinity, all the samples were annealed at 500 °C for 2 h under oxygen atmosphere.

Characterization

X-ray diffraction (XRD) pattern of samples were recorded using X-ray diffractometer (SEIFERT—2002 Model, DYEFLAX, Germany) with Cu Kα radiation. Morphology of the samples was analyzed by FESEM S-4800 Hitachi model scanning electron microscopy (SEM). The optical measurements were carried out using Shimadzu UV 2450 spectrophotometer equipped with an integrated sphere assembly ISR-240A. Room temperature photoluminescence (PL) measurements were carried out on a Fluorolog-3 spectrometer. Hall effect measurements were done using an Ecopia Hall effect (HMS 5000) system. To measure electrical properties of the samples, thin pellets (thickness—0.2 mm, pressure—10 ton) were made from powder samples using hydraulic press. Ohmic contacts were made on the pellets with silver paste at the edges of four corners to maintain Vander Pauw configuration.

Results and discussion

Structural analysis

The structural parameters and phase purity of the undoped and the Cs-doped ZnO NPs at different concentration were estimated using XRD (Fig. 1a). All the diffraction peaks are indexed with standard ZnO data (JCPDS 36-1451). Prominent diffraction peaks such as (100), (002), (101) patterns from all annealed samples correspond to polycrystalline ZnO with hexagonal wurtzite structure [12]. No secondary peak corresponding to Cs was observed. XRD results confirmed that Cs 1 mol% doped ZnO showed enhanced crystallinity, which indicates inclusion of Cs in ZnO matrix is more effective in Cs 1 mol%:ZnO NPs and with further increase in concentration the crystallinity is observed to decrease, which may be due to agglomeration. In order to observe the effect of Cs doping, an enlarged version of XRD patterns is shown in Fig. 1b. It is obviously seen from the figure (Fig. 1b) that the predominant peaks (100), (002), and (101) are shifted toward lower angle side, suggesting the inclusion of Cs ions into ZnO matrix in accordance with Vegard's law. The ionic radius of Cs^{+} ion (167 pm) is much larger than Zn^{2+} ions (74 pm) and it is well known that if the ionic size of the dopant is larger than the host, the XRD peak tend to shift toward lower angle. A similar phenomenon has been observed elsewhere in ZnO doped with *p*-type dopant [12, 13].

Crystallite size was calculated from the well-known Debye–Scherrer equation. Crystallite size, lattice parameter, and stain of the samples are summarized in Table 1. The estimated crystallite size as a function of Cs doping increases from 40 to 52 nm, due to the fact, that the larger ionic size of Cs cation induces grain growth. A slight reduction in lattice parameter value suggests heterogeneous nucleation as well as a decrease in the lattice strain is observed with inclusion of Cs ions (Table 1). Similar effects were observed by Kumar et al. [22] in Ni-doped CeO_2 NPs. Thus the decrease in lattice parameter and lattice strain in the current study suggests substitution of Cs in ZnO matrix.

Morphology analysis

Figure 2a shows the SEM images of undoped and Cs-doped ZnO NPs. In the earlier report, we found alcohol

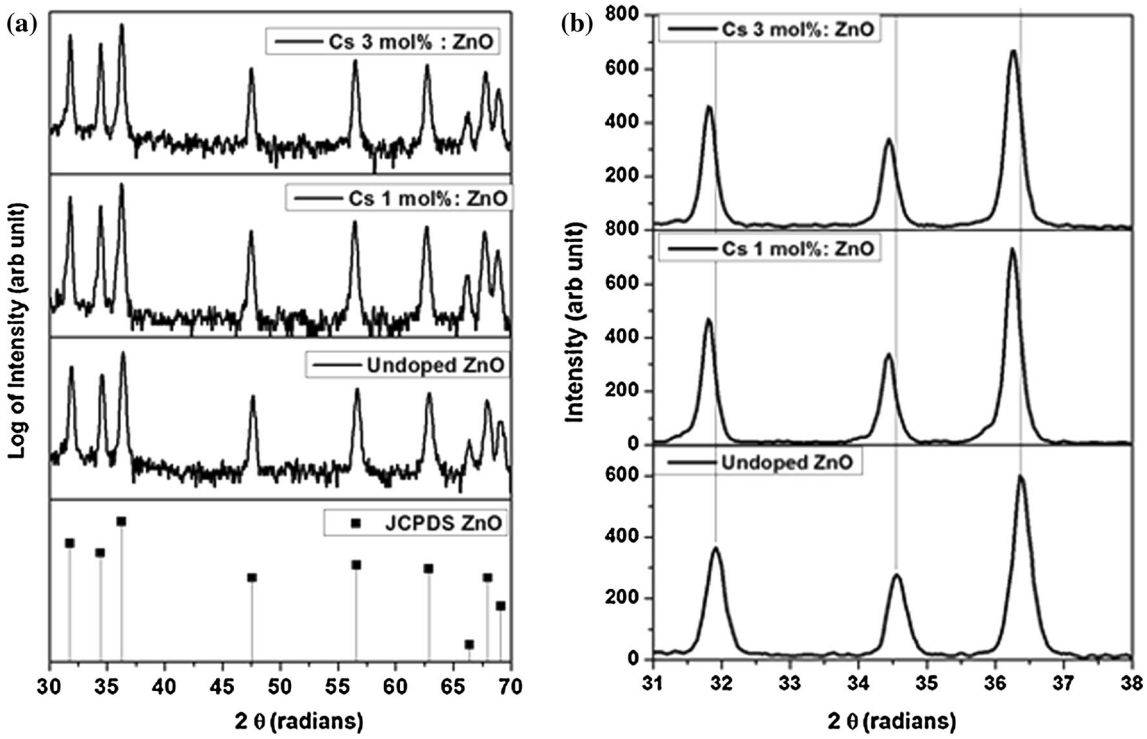

Fig. 1 **a** XRD spectra of undoped and Cs-doped ZnO NPS, **b** enlarged XRD pattern of undoped and Cs-doped ZnO NPs

Table 1 Lattice parameter, crystallite size, and strain values for undoped and Cs-doped ZnO NPs

Samples	Crystallite size (nm)	Lattice parameter (Å)		Strain ($\times 10^{-3}$)	Volume (cm^3)
		a	*c*		
JCPDS (36-1451)		3.253	5.209		
Undoped ZnO	40.05	3.2478	5.206	1.406	47.557
Cs 1 mol% doped ZnO	52.414	3.2456	5.2032	0.9393	47.47
Cs 3 mol% doped ZnO	52.404	3.2448	5.204	0.94	47.44

derived ZnO NPs showed pyramid shaped particles whereas green synthesized ZnO NPs showed triangular-shaped particles. It is observed that the particle size is reduced and morphology change is observed due to effect of "green-solvent" [20]. It was evidenced from the Fig. 2a, that triangular-shaped particles were observed in both ZnO- and Cs-doped ZnO samples and an increase in particles size with Cs concentration is noticed. It is also observed from the Fig. 2a, that increase in dopant concentration induces agglomeration which is in concurrence with reduction in crystallinity at higher dopant concentration due to agglomeration (XRD pattern Fig. 1b). Energy dispersive X-ray (EDX) analysis shown in Fig. 3 confirms inclusion of Cs ion in ZnO lattices.

Optical analysis

Transmission spectra of the undoped and Cs-doped ZnO NPs are shown in Fig. 4a. From the spectra, it is clear that all NPs exhibit a transmission of about 85 % in the visible range and subsequently has increased with dopant concentration. The effect of Cs on band gap energy is analyzed using UV–visible absorption analysis. The characteristic adsorption band edge of ZnO is red shifted with increase in Cs concentration in ZnO:Cs samples (inset Fig. 4a). It may be due to the surface effect and quantum confinement effect [23]. The observed enhancement in blue shift band edge with increasing Cs content indicates the incorporation of Cs ions into the Zn site in the ZnO lattice.

The energy band gap (E_g) was determined by well-known Tauc equation [24]. Figure 4b shows the plot of $(\alpha h\gamma)^2$ versus $h\gamma$, where α is the optical absorption coefficient and $h\gamma$ is the energy of the incident photon. The E_g values are 3.12, 3.09, and 3.08 for the undoped, 1 and 3 %, Cs-doped ZnO NPs, respectively. Change in morphology and size due to green-solvent may be one of the reasons in reduction of bandgap. In this study, the reduction in band gap is attributed to effect of green-solvent, size effect, and oxygen vacancy. Band gap narrowing was observed for

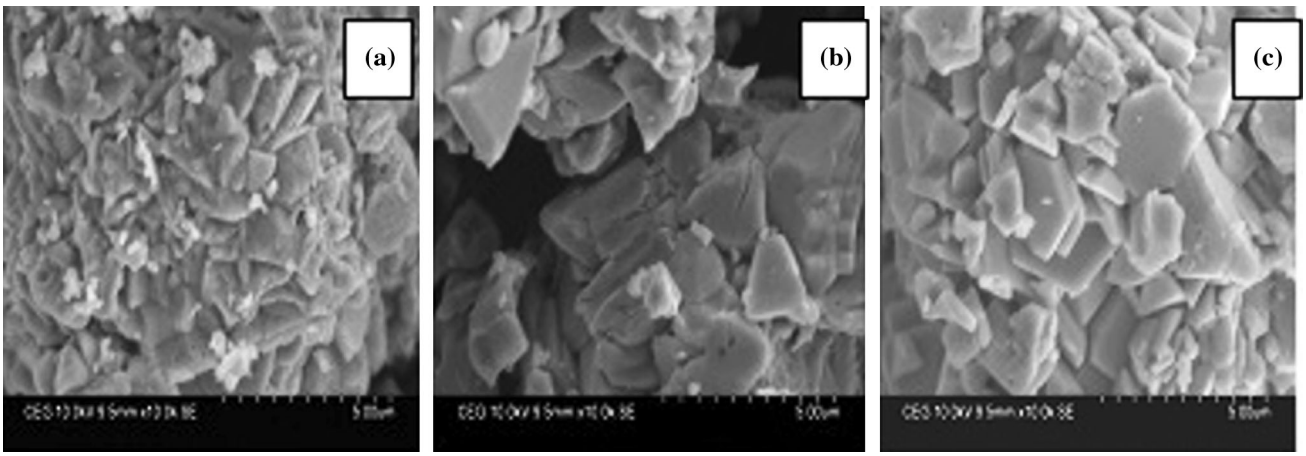

Fig. 2 SEM images of **a** undoped, **b** 1 mol% Cs: ZnO, and **c** 3 mol% Cs: ZnO NPs

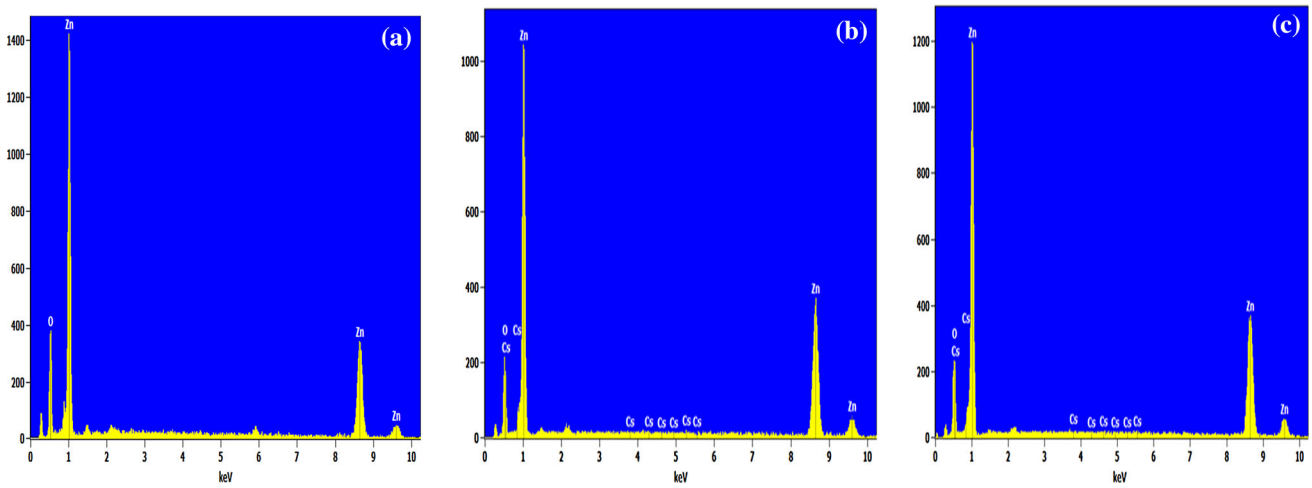

Fig. 3 EDS images of **a** undoped **b** 1 mol% Cs:ZnO, and **c** 3 mol% Cs:ZnO NPs

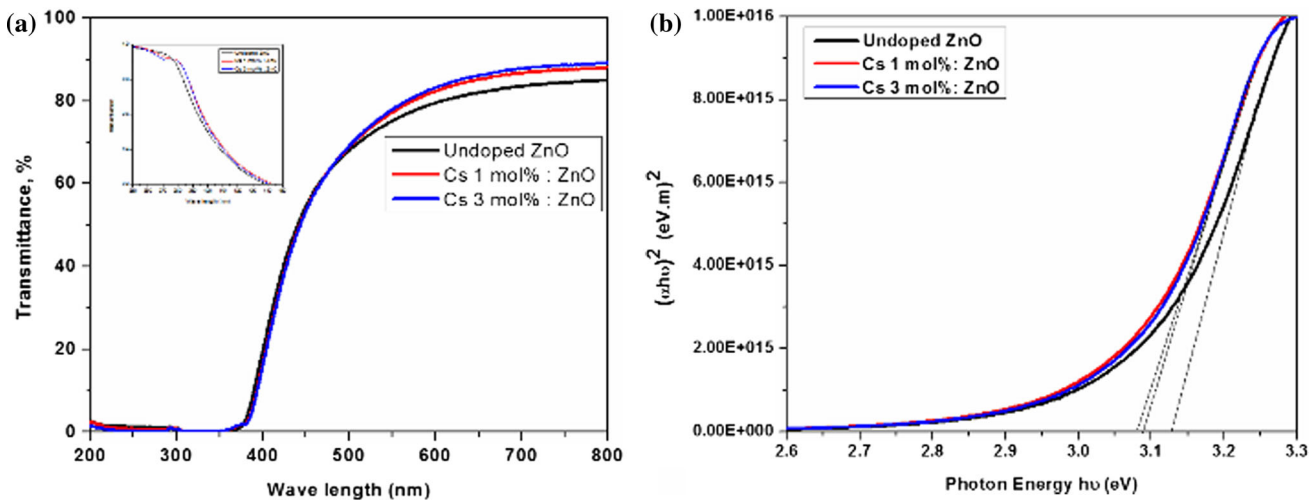

Fig. 4 **a** Transmittance spectra of undoped and Cs-doped ZnO NPs, *inset figure* enlarged view of band edge shift in absorbance spectra, **b** plot of $(\alpha h\gamma)^2$ versus $h\gamma$

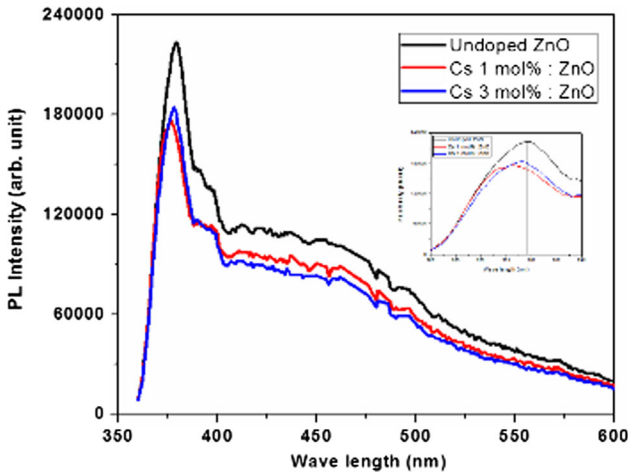

Fig. 5 Room temperature PL spectra of undoped and Cs-doped ZnO NPs annealed at 500 °C, 2 h under O_2 atmosphere (*inset figure* magnified view of PL peak shift)

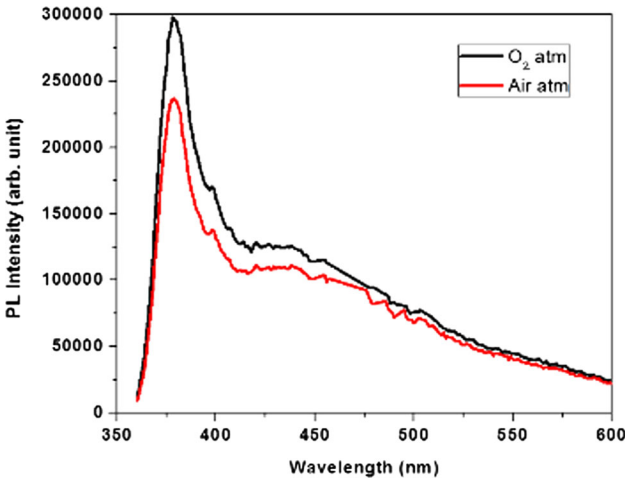

Fig. 6 Room temperature PL spectra of Cs 1 mol%: ZnO NPs annealed at 700 °C, 2 h under O_2 and air atmosphere

Cs-doped ZnO samples. Generally reduction in bandgap can be explained by two ways, one is size effect and another one is dopant concentration. It is well known that the increase in crystallite size will decrease the band gap [9, 24]. XRD and SEM results of present study indicate an increase in particle size with inclusion of Cs. Usually, a widening of the bandgap is observed for ZnO doped with donors; while a bandgap reduction is observed if doped with acceptors (i.e., *p*-type ZnO) due to the formation of impurity band inside the forbidden gap region [6]. Thus the band gap shrinkage observed in Cs-doped ZnO particles can be attributed to size effect as well as to dopant effect. Bandgap reduction also suggests the possibility of *p*-type behavior in the Cs-doped ZnO samples.

Photoluminescence studies

The photo luminescence study is a powerful tool for investigating effect of impurity doping in ZnO nanostructures. Figure 5 shows room temperature PL emission spectra of undoped and Cs-doped ZnO NPs under 320 nm excitation. The emission spectra consist of two main peaks, a sharp peak at 379 nm in the UV region and a broad peak around 450 nm in the visible region. The observed UV emission is attributed to excitonic recombination of near band edge emission in ZnO and the blue emission may be due to Zn interstitial/surface defects [25]. Kshirsagar et al. [26] reported the blue emission in ZnO due to acceptor bound exciton. Lü et al. [27] has reported that the blue emission is associated with Zn vacancy and Zn interstitial defects.

In the present study, reduction in PL emission intensity is observed for Cs-doped ZnO NPs. This can be explained from the net charge value, i.e., if the net charge of the slightly ionized oxygen vacancy in ZnO is negative, it creates an acceptor state by pushing the valance band levels higher into the bandgap [28]. Also doped cation provides competitive pathways for recombination, which results in quenching of emission intensity.

It is evident from the Fig. 5 (inset figure), that a blue shift is observed in the Cs-doped samples compared to the undoped ZnO. Thangavel et al. have reported blue shift with inclusion of Cs ions and attributed it to band filling effect of free carriers. Similar results were observed for Li-doped ZnO thin films deposited by PLD [28]. UV emission peak is observed to shift toward lower wave length side with decreasing Cs concentration. However, it is interesting to note in our experiment that the shift is more predominant in Cs 1 mol% and also the UV emission peak observed at 375 nm in Cs 1 mol% doped ZnO is less intense. Thus the results indicate that the Cs doping can slightly modify the band gap of ZnO and also illustrate that doping can influence the optical properties in ZnO NPs. Hence to analyze the annealing effect in Cs 1 mol% doped ZnO, the annealing temperature was increased from 500 to 700 °C under oxygen and air atmosphere were used for analysis. Figure 6 shows the characteristic PL spectrum Cs 1 mol% doped ZnO annealed at 700 °C for 2 h under O_2 and air atmosphere. It is obvious from the Fig. 6 that the annealing of Cs 1 mol% doped ZnO NPs at 700 °C in oxygen atmosphere enhanced the UV emission, while decrease in UV emission is observed when the sample is annealed in air. In this O-rich condition, the amount of oxygen that diffuses into the sample is high and the concentration of oxygen vacancies decreases [29].

Electrical measurements

The electrical properties of the undoped and Cs-doped samples are shown in Table 2. It was evidenced from the

Table 2 Electrical properties of undoped ZnO and Cs-doped ZnO NPs

Samples	Carrier type	Carrier concentration (cm^{-3})	Mobility, μ (cm^2/V s)	Average Hall coefficient (cm^3/C)
ZnO	*n*	-7.49×10^{18}	5.28	-2.12×10^{1}
Cs 1 mol% doped ZnO	*p*	1.3×10^{18}	7.3	2.18×10^{2}
Cs 3 mol% doped ZnO	*p*	3.56×10^{17}	5.99	6.13×10^{2}

Table 2, undoped ZnO shows *n*-type conduction with a carrier concentration of $-7.49 \times 10^{18}/cm^3$. Cs is a group I element, thus it has the potential to be a deep acceptor in Cs-doped ZnO. These results indicate, Cs act as a deep acceptor in the present Cs-doped ZnO samples and the hole concentration decreased with increase in Cs concentration. The data shows that the doping of 1 mol% Cs in ZnO shows higher carrier concentration than Cs 3 mol% doped ZnO. The reduction in hole concentration with increasing dopant concentration (more than 1 mol%) may be attributed to limitation in dopant solubility in ZnO lattices [15]. Thus the optimum concentration is found to be Cs 1 mol% with a high mobility of 7.3 cm^2/V s, a maximum hole concentration of $1.3 \times 10^{18}/cm^3$ and a positive Hall coefficient of 2.18×10^2 cm^3/C. These results confirm effective substitution of Cs in Zn sites and it act as a deep acceptor, which leading to *p*-type conductivity in Cs-doped ZnO NPs.

Conclusion

In this work, Cs-doped ZnO of different Cs concentrations (1, 3 mol%) were synthesized by eco-friendly green route and the effect of Cs concentration was analyzed. XRD results confirmed that NPs have polycrystalline and hexagonal wurtzite structure. Better crystallinity was observed for Cs 1 mol%:ZnO NPs as well as crystallite size increases with Cs concentration. SEM result shows triangular-shaped NPs and the particles are highly agglomerated with dopant concentration. Optical analysis revealed, band edge shifted toward higher wavelength. Hence, from the results, it is concluded that there is a reduction in band gap with inclusion of Cs ions in ZnO matrix. The PL spectra showed characteristic UV emission at 379 nm and defect induced blue emission around 450 nm. The observed blue shift of the optical band gap and quenching of bandedge emission are attributed to dopant effect and the net charge carrier value (−ve). Enhanced UV emission for the annealed samples at higher temperature (700 °C) under oxygen atmosphere confirmed the charge compensation. Hall measurement results showed *p*-type conductivity in Cs-doped ZnO NPs, to the fact that Cs forms deep acceptor level in substitutional Zn site. From the above results, it may be concluded that the 1 mol% Cs in ZnO is an optimum concentration. The correlation between the conductivity type and near bandedge peak shift with doping induced bandgap changes suggest *p*-type conduction in Cs-doped ZnO NPs.

Acknowledgements This work is mainly supported by the research funds from the management of Hindustan University through CENCON. One of the authors NGS acknowledges research funding from Dongguk University though QSRC and NITA. This research was also supported by Leading Foreign Institute Recruitment Program through the National Research Foundation of Korea (NRF) funded by the Ministry of Education, Science and Technology (MEST) (No. 2013-044975) and by the International Research & Development Program of the National Research Foundation of Korea (NRF) funded by the Ministry of Education, Science and Technology (MEST) of Korea (Grant Number: 2012-033431). Author sincerely thanks, Dr. M.T Jose, Head Radiation safety Division, IGCAR Kalpakkam for photoluminescence measurements.

References

1. Yamajo N, Nunokawa R, Sugiyama K (1994) Customer network with a highly reliable design method using short-wavelength electro-optical devices and optical fibers. IEEE T Consum Electr 40(3):580–586
2. Orton JW, Foxon CT (1998) Group III nitride semiconductors for short wavelength light-emitting devices. Rep Prog Phys 61:1–75
3. Mokkapati Sudha, Jagadish Chennupati (2009) III–V compound SC for optoelectronic devices. Mater Today 12(4):22–32
4. Özgür Ü, Alivov C, Liu C, Teke A, Reshchikov A, Doğan S, Avrutin V, Cho S-J, Morkoç H (2005) A comprehensive review of ZnO materials and devices. J Appl Phys 98(041301):1–72
5. Look DC (2001) Recent advances in ZnO materials and devices. Mater Sci Eng B 80:383–387
6. Gupta MK, Sinha N, Kumar B (2011) *p*-type K-doped ZnO nanorods for optoelectronic applications. J Appl Phys 109(083532):1–5
7. Pan XH, Jiang J, Zeng YJ, He HP, Zhu LP, Ye ZZ, Zhao BH (2008) Electrical and optical properties of phosphorus-doped *p*-type ZnO films grown by metal organic chemical vapor deposition. J Appl Phys 103(023708):1–4
8. Yan YF, Li JB, Wei S-H, Al-Jassim MM (2007) Possible approach to overcome the doping asymmetry in wide bandgap semiconductors. Phys Rev Lett 98(135506):1–4
9. Thomas MA, Cui JB (2010) Electrochemical route to *p*-type doping of ZnO nanowires. J Phys Chem Lett 1(7):1090–1094
10. Liu W, Xiu F, Sun K, Xie Y-H, Kang L, Wang YW, Zou J, Yang Z, Liu J (2010) Na-doped *p*-type ZnO microwires. J Am Chem Soc 132(8):2498–2499
11. Lv J, Huang K, Chen X, Zhu J, Wang L, Song X, Sun Z (2011) Effect of preheating temperatures on microstructure and optical

properties of Na-doped ZnO thin films by sol–gel process. Superlattice Microstruct 49(4):477–486
12. Rauch C, Gehlhoff W, Wagner MR, Malguth E, Callsen G, Kirste R, Salameh B, Hoffmann A, Polarz S, Aksu Y, Driess M (2010) Lithium related deep and shallow acceptors in Li-doped ZnO nanocrystals. J Appl Phys 107(024311):1–5
13. Kushnirenko VI, Markevich IV, Zashivailo TV (2012) Acceptor related to group I element in ZnO ceramics. J Lumin 132:1953–1956
14. Vettumperumal R, Kalyanaraman S, Thangavel R (2013) Enhancement of optical conductivity in the ultra-violet region of Cs doped ZnO sol gel thin films. J Sol Gel Sci Technol 66:206–211
15. Thangavel R, Singh Moirangthem R, Lee WS, Chang YC, Wei P-K, Kumar J (2010) Cesium doped and undoped ZnO nanocrystalline thin films: a comparative study of structural and micro-Raman investigation of optical phonons. J Raman Spectrosc 41:1594–1600
16. Lee J, Choi W, Kim C, Hong J (2006) Electrical and optical properties of a *n*-type ZnO thin film deposited on a Si substrate by using a double RF co-sputtering method. J Korean Phys Soc 49:1126–1129
17. Kumar SS, Venkateswarlu P, Rao VR, Rao GN (2013) Synthesis, characterization and optical properties of zinc oxide nanoparticles. Int Nano Lett 3(30):1–6
18. Ni Y, Wei X, Hong J, Ye Y (2005) Hydrothermal synthesis and optical properties of ZnO nanorods. Mater Sci Eng B 121(1–2):42–47
19. Sangeetha G, Rajeshwari S, Venckatesh R (2011) Green synthesis of zinc oxide nanoparticles by *Aloe barbadensis* miller leaf extract: structure and optical properties. Mater Res Bull 46:2560–2566
20. Raman S, Regupathy V, Krishnaswamy S, SenthilKumaar S, Ganapathi Subramanian N, Kang TW (2013) Green catalyst of nano zirconia doped ZnO: synthesis, characterization and photomineralization under UV/visible light TMS2013. Suppl. Proc., 87–95
21. Ragupathi V, Raman S, Krishnaswamy S, Sada S, Nagarajan GS (2013) Symposium—novel solution routes for nano/biomaterials: ICMAT 2013
22. Kumar S, Kim YJ, Koo BH, Lee CG (2010) Structural and magnetic properties of Ni doped CeO2 nanoparticles. J Nanosci Nanotechnol. 11:7204–7207
23. Lin K-F, Cheng H-M, Hsu H-C, Lin L-J, Hsieh W-F (2005) Band gap variation of size-controlled ZnO quantum dots synthesized by sol–gel method. Chem Phys lett 409:208–211
24. Changle Wu, Huang Qingli (2010) Synthesis of Na doped ZnO nanowires and their photocatalytic properties. J Lumin 130:2136–2141
25. Zeng H, Duan G, Li Y, Yang S, Xu X, Cai W (2010) Blue luminescence of ZnO nanoparticles based on non-equilibrium processes: defect origins and emission controls. Adv Funct Mater 20:561–572
26. Kshirsagar SD, Nikesh VV, Mahamuni S (2006) Exciton structure in sodium doped zinc oxide quantum dots. Appl Phys Lett 89(053120):1–3
27. Lü J, Huang K, Zhu J, Chen X, Song X, Sun Z (2010) Preparation and characterization of Na-doped ZnO thin films by sol–gel method. Phys B 405(15):3167–3171
28. Li G, Sambasivam S, Kim SB, Park SW, Choi BC, Jeong JH (2011) Structural, morphological, and optical studies on Li-doped ZnO thin films deposited by using PLD. J Korean Phys Soc 59(4):2770–2773
29. Hur T-B, Yoo D-H, Jeen GS, Hwang Y-H, Kim H-K (2003) The effects of thermal annealing of ZnO ceramics. J Korean Phys Soc 42:S1283–S1286